PEER REVIEW, Vol. 6, Nº 15, 2024
DOI: 10.53660/PRW-2467-4525
ISSN: 1541-1389

Metallurgical Study of Manganese Lump ores from Minas Gerais, Brazil

Adriana Baldessin Costa
ORCID: https://orcid.org/0009-0005-2848-1330
Universidade Federal de Ouro Preto, Brasil
E-mail: abc_emin@yahoo.com.br
Tiany Guedes Cota
ORCID: https://orcid.org/0000-0002-5845-0990
Universidade Federal do Ceará, campus Cratéus, Brasil
E-mail: tianycota@crateus.ufc.br
Francielle Câmara Nogueira
ORCID: https://orcid.org/0000-0001-5912-011X
Universidade Federal de Ouro Preto, Brasil
E-mail: francielle.nogueira@ufop.edu.br
Rosa Malena Fernandes Lima
ORCID: https://orcid.org/ 0000-0002-0326-1797
Universidade Federal de Ouro Preto, Brasil
E-mail: rosa@ufop.edu.br
Érica Linhares Reis
ORCID: https://orcid.org/ 0000-0003-3760-9904
Universidade Federal de Ouro Preto, Brasil
E-mail: erica@ufop.edu.br
Hernani Mota de Lima
ORCID: https://orcid.org/ 0000-0002-5595-4149
Universidade Federal de Ouro Preto, Brasil
E-mail: hernani.lima@ufop.edu.br

ABSTRACT

This study investigates the correlation between the type and quality of manganese lumps ore (- 19.0 + 6.3 mm) and its metallurgical behavior from two distinct mines located in Minas Gerais, Brazil. Physical, chemical, and mineralogical characterization, along with metallurgical tests such as drumming and decrepitation, were conducted on samples designated as GPN (Penedo) and GTT (Totonho). Significant variations in manganese, iron, and silica levels were observed. High silica values suggest potential suitability for SiMn production. Main crystalline phases identified were spessartite, todorokite, pyrolusite, cryptomelane, quartz, dolomite, and goethite. Drumming and decrepitation tests showed a tendency for fines generation, especially in the -6.3 mm fraction, due to high porosity and the presence of hydrated minerals. Decrepitation indices were lower for dried or heat-treated samples, with reductions of 31% for GTT and 43% for GPN when dried at 105°C. Decrepitation results highlighted the significant impact of moisture on fines generation.

Keywords: Manganese ore; Characterization; Metallurgical behavior; Drumming tests; Decrepitation tests.

Recebido: 15/07/2024 | Aceito: 21/08/2024 | Publicado: 25/08/2024

RESUMO

Este estudo investiga a correlação entre o tipo e a qualidade do minério de manganês na fração *lump ore* (- 19,0 + 6,3 mm) e seu comportamento metalúrgico de amostras provenientes de duas minas localizadas em Minas Gerais, Brasil. Foram realizadas caracterizações física, química e mineralógica, além de testes metalúrgicos como tamboramento e crepitação, nas amostras denomidas GPN (Penedo) e GTT (Totonho). Observou-se variação nos teores de manganês, ferro e silica, com altos valores de sílica indicando potencial para a produção de SiMn. As principais fases cristalinas identificadas foram espessartita, todorokita, pirolusita, criptomelana, quartzo, dolomita e goethita. Os testes de tamboramento e crepitação mostraram uma tendência para a geração de finos, especialmente na fração - 6,3 mm, devido à alta porosidade e à presença de minerais hidratados. Os índices de crepitação foram menores para amostras secas ou tratadas termicamente, com reduções de 31% para GTT e 43% para GPN quando secas a 105°C. Os resultados de decrepitação destacaram o impacto significativo da umidade na geração de finos.

Palavras-chave: Minério de manganês; Caracterização; Comportamento metalúrgico; Testes de tamboramento; Testes de crepitação.

INTRODUCTION

Manganese is a crucial element in the ferroalloys industry, with about 90-95% of all produced manganese being used in steel production (Cheraghi et al., 2020; IMnI, 2016; Liu, 2019). On average, approximately 10 kg of manganese is consumed per ton of steel. The addition of manganese to steel serves multiple purposes, including enhancing the steel's mechanical properties and assists in controlling sulfur and oxygen during the refining process (Oslen et al., 2007; Tangstad, 2013; Cota et al., 2023).

Manganese ferroalloys are typically manufactured using an electric submerged arc furnace (Peterson et al., 2020). In these furnaces, the carbothermic reduction of ore compounds occurs through the use of a reducing agent. The physical, chemical, and mineralogical properties of manganese ores significantly influence the operational performance of steel reactors. These properties determine the quality of the alloys, the volume and composition of the slag, and the metallic yield. They also affect the behavior and efficiency of internal chemical reactions. Furthermore, variations in these properties can lead to increased specific energy consumption, reducer consumption, and production costs (Olsen et al., 2007; Faria et al., 2010; Faria et al., 2012; Coetsee et al., 2015; Grishchenko et al., 2015; Digernes et al., 2018).

Even when extracted from the same deposit, variations in ore properties can adversely affect the efficiency of treatment plants and metallurgical processes (Porphírio et al., 2010). Therefore, establishing quality indicators through geometallurgical characterization is necessary to ensure product homogeneity and maintain furnace productivity. By understanding these ore characteristics, it is possible to optimize the economic exploitation, including its extraction, beneficiation, and the allocation of resources and investments, to maximize recovery and meet market quality demands (Berg and Olsen, 2000; Faria et al., 2008; Faria et al., 2010; Chemale Jr. and Takehara, 2013; Ringdalen et al., 2015; Singh et al., 2016).

Pioneering studies by Faria et al. (2008), Viana (2009), Reis (2010), Sonrensen et al. (2010), Faria et al. (2011), Faria et al. (2012), and Faria et al. (2013) have developed methods for characterizing and analyzing the metallurgical behavior of different manganese ore types in Brazil. These studies aim to predict the quality of manganese ore during transportation, handling, and furnace operations, enabling the creation of more suitable blends for charge production, compliance with product specifications, and maximization of furnace yield and productivity.

In this context, the main objective of this work is to present a characterization of the manganese lump ores from two mines in Minas Gerais, Brazil. By establishing numerical reference parameters based on the results of physical, chemical, and mineralogical analyses, this study enables the efficient utilization of manganese present in these deposits.

MATERIAL AND METHODS

In this study, manganese ore samples were sourced from two distinct mines located in Minas Gerais, Brazil. The specific lump ores analyzed were designated as GPN (Penedo lump ore) and GTT (Totonho lump ore). Chemical analyses were performed with titrimetry for the major elements and Inductively Coupled Plasma Optical Emission Spectroscopy (ICP/OES) for the minor elements. X-ray diffraction (XRD) analysis was performed using the X'PERT³ equipment, employing the total powder method with a scan rate of 1.2º /min. Mineralogical analyses were conducted using optical microscopy, employing both transmitted and reflected light microscopy techniques to examine opaque and transparent minerals. Optical microscopy was performed using the LEICA metallographic microscope.

The density of the material was measured using a helium gas pycnometer (Ultrapyc Nova 1200e - Quantachrome), achieving a standard deviation of 0.05%. Specific surface area and porosity were determined utilizing a gas adsorption analyzer (Nova 1200e) under a nitrogen atmosphere, employing the BET method for specific surface area analysis. Thermogravimetric analysis (TGA) was conducted using a thermobalance. Samples were heated at a rate of 10ºC/min from an initial temperature of 25ºC to a final temperature of 1000ºC under a nitrogen atmosphere.

All samples, prior to the drumming and decrepitation tests, were subjected to dry sieving using a 6.3mm Tyler sieve to remove residual fines. After sieving, the samples were homogenized and quartered to ensure representativeness in subsequent analyses.

The decrepitation index was measured according to ISO 8731 (2004), the standard method for iron ore, in a muffle furnace at 700 °C. This method was adapted based on previous studies by Faria et al. (2010) and Faria et al. (2013) for manganese ores. The particle size range (19.0 to 6.3 mm) with an average particle size of 12.7 mm chosen for the decrepitation tests is commonly used in submerged arc furnaces. Decrepitation tests were performed using two stainless steel containers equipped with lids for material

storage and an electric oven. Samples were analyzed in their natural moisture state, dried at 105ºC, and after undergoing heat treatment. The experimental temperature ramped up at a constant rate of 5ºC/min in an uncontrolled atmosphere, starting from room temperature and reaching 700°C, maintained for 30 minutes. Samples subjected to heat treatment underwent a preliminary 48 hours conditioning at 200ºC. Crackle rates were determined based on the percentages of fines passing through the 6.3mm, 3.35mm, and 0.500mm via dry sieving.

The drumming tests were performed according to ISO 3271 standard, with adaptations based on the previous research by Faria et al. (2013). The optimal lump size for each manganese ore sample was evaluated using a system equipped with adjustable rotation capabilities. The drumming tests included interruptions at 10, 20, and 30 minutes, with a frequency of 510.6 Hz and a rotation speed of 30 rpm. Cold granulometric degradation (CGD) indices were evaluated to examine fine evolution, determined by the mass percentages within the 6.3mm, 3.35mm, and 0.500mm size ranges via dry sieving.

RESULTS AND DISCUSSION

Chemical characterization

The Table 1 shows the chemical analysis of the particle size range between 19 and 6.3 mm. The manganese ores studied presented distinct chemical characteristics. The GTT exhibited levels of Mn and SiO_2 higher than GPN. Conversely, the Fe content of GTT is lower than that of GPN. Both samples of manganese lump ore had results for the levels of Al_2O_3 and LOI above 10%. The levels of P, Ba, Ti, and K did not show significant variations between the mines.

Table 1 - Chemical analysis of the manganese lump ores in the range between 19 and 6.3 mm

Sample	%Mn	%Fe	%SiO_2	%Al_2O_3	%P	%Ba	%Ti	%K	%CaO	%MgO	%LOI
GTT	30.8	5.1	26.0	11.5	0.1	0.2	0.2	0.2	1.1	1.4	11.9
GPN	24.5	11.0	21.0	11.8	0.1	0.2	0.2	0.3	1.6	1.3	12.4

LOI: Loss on ignition at 1000 °C.

An important parameter to consider in the materials fed into the electric furnace is the manganese-to-iron ratio (Mn/Fe), as it directly influences the manganese content in the final product. The Mn/Fe ratio for GTT and GPN was 6.0 and 2.2, respectively. Therefore, ores from different sources could be blended to obtain the optimal ratio and control elements such as silica, alumina, and phosphorus (Ullmann, 1985; Cota et al., 2023). Additionally, it is important to highlight the high silica values in the samples studied, which may indicate their suitability for use in SiMn production.

Mineralogical characterization

The main crystalline phases identified in the X-ray diffraction analyses were spessartite, todorokite, pyrolusite, cryptomelane, quartz, dolomite, and goethite. Figure 1 shows micrographs of GPN samples (a-c), obtained with a reflected light optical microscope, and a micrograph of GTT samples (d-e), obtained with a transmitted light optical microscope. Cryptomelane is observed in the lower part of the mineral, exhibiting a cryptocrystalline texture with fractures, while the upper part appears to be an alteration of the cryptomelane edge (Fig. 1a). This alteration has a porous appearance and strong anisotropy, potentially being the mineral pyrolusite. According to Sorensen et al. (2010), pyrolusite is usually a product of the extreme oxidations suffered by todorokite or cryptomelane. A todorokite crystal can be observed with a medium to dark gray coloration, distinct bireflectance, and fibrous crystals in porous aggregates (Fig. 1b). This mineral characteristic commonly occurs due to the alteration of primary manganese minerals. Goethite appeared gray with a weak bluish tone, exhibiting no bireflectance, and was found in association with translucent minerals (Fig. 1c). Grains of spessartine (Fig. 1d) and quartz (Fig. 1e) can be noted. Spessartine ($Mn_3Al_2Si_3O_{12}$) is a manganese silicate mineral often associated with quartz (Navarro and Zanardo, 2018). As can be seen the mines exhibit a predominance of manganese silicate and hydroxide minerals.

Figure 1 - Photomicrography of the manganese lump ore samples

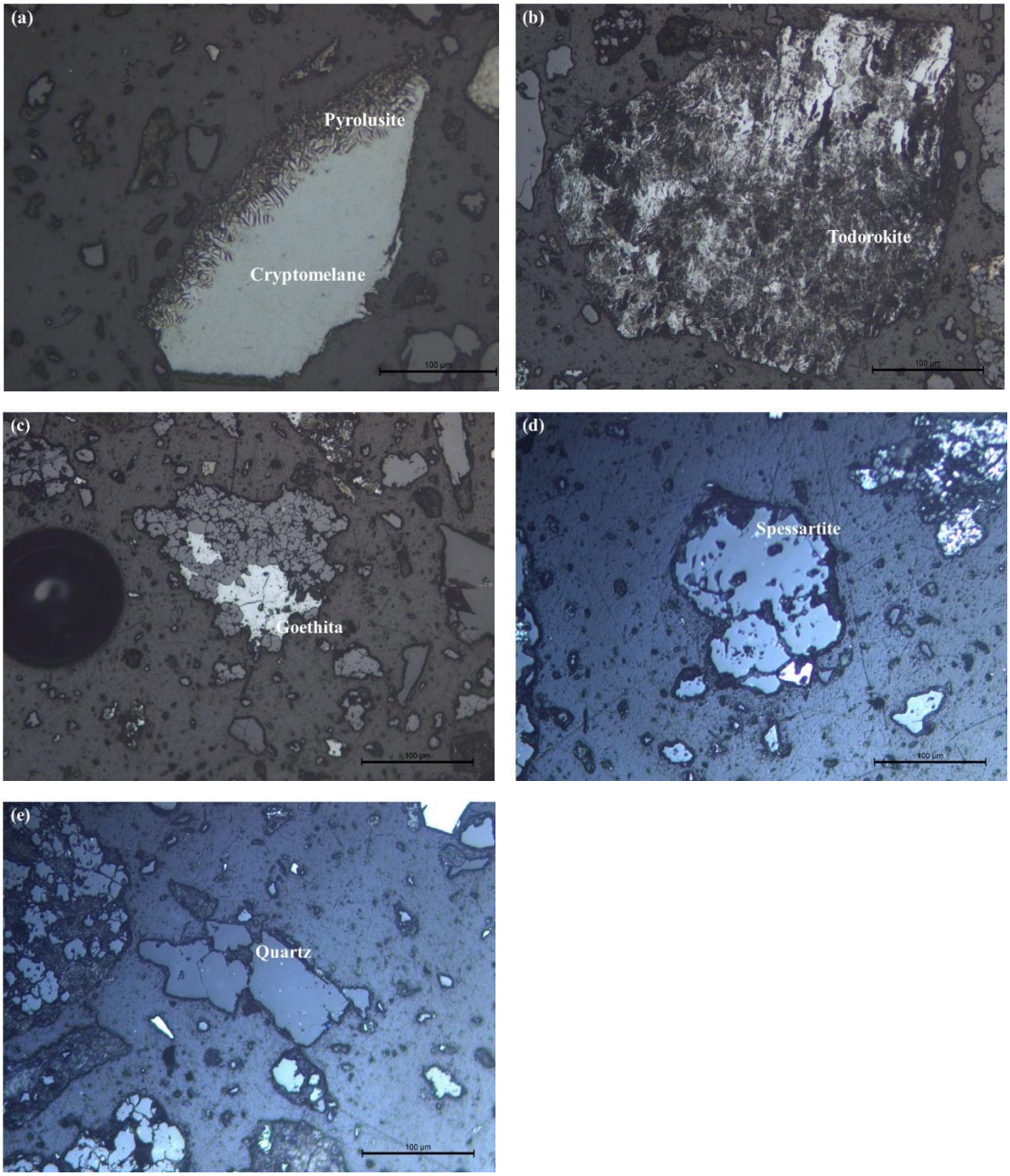

Porosimetry

Table 2 shows the results of density, surface area and porosity for the studied manganese lump ores.

Table 2 - Pycnometry and BET parameters for manganese lump ores

Sample	Density (g/cm^3)	Specific surface area (m^2/g)	Total pore volume (cm^3/g)	Porosity (%)
GTT	3.7	20.4	0.010	3.6
GPN	3.5	36.6	0.020	6.2

The GPN sample exhibits higher specific surface area, porosity, and total pore volume than the GTT sample. Compared to the results of Faria et al. (2012) for three different manganese lump ores in Brazil, the GTT and GPN samples showed higher specific surface area values. This indicates a possible difference in the geological characteristics of these ores.

The higher specific surface area and total pore volume of the GPN sample indicate a more porous structure with a larger exposed surface. This increased porosity could be due to the presence of cracks and fractures on the mineral surface, possibly caused by more porous and hydrated manganese or iron minerals.

Porosity data is crucial for ferroalloy production, especially for manganese ores. Previous studies, such as those conducted by Faria et al. (2012), have established a correlation between the total volume of pores and the intensity of decrepitation in manganese ores, finding that a greater pore volume correlates with a heightened decrepitation intensity.

Thermogravimetry

Figure 2 shows the thermogravimetry curves of the manganese lump ores. Thermogravimetry analysis has shown that GTT and GPN had mass losses primarily due to the elimination of structural water from the hydrated todorokite and goethite phases, as well as the thermal decomposition of pyrolusite and cryptomelane oxides. Additionally, the decomposition of calcium and magnesium carbonate from dolomite contributed to the mass loss.

Figure 2 - Thermogravimetric curves for manganese lump ores

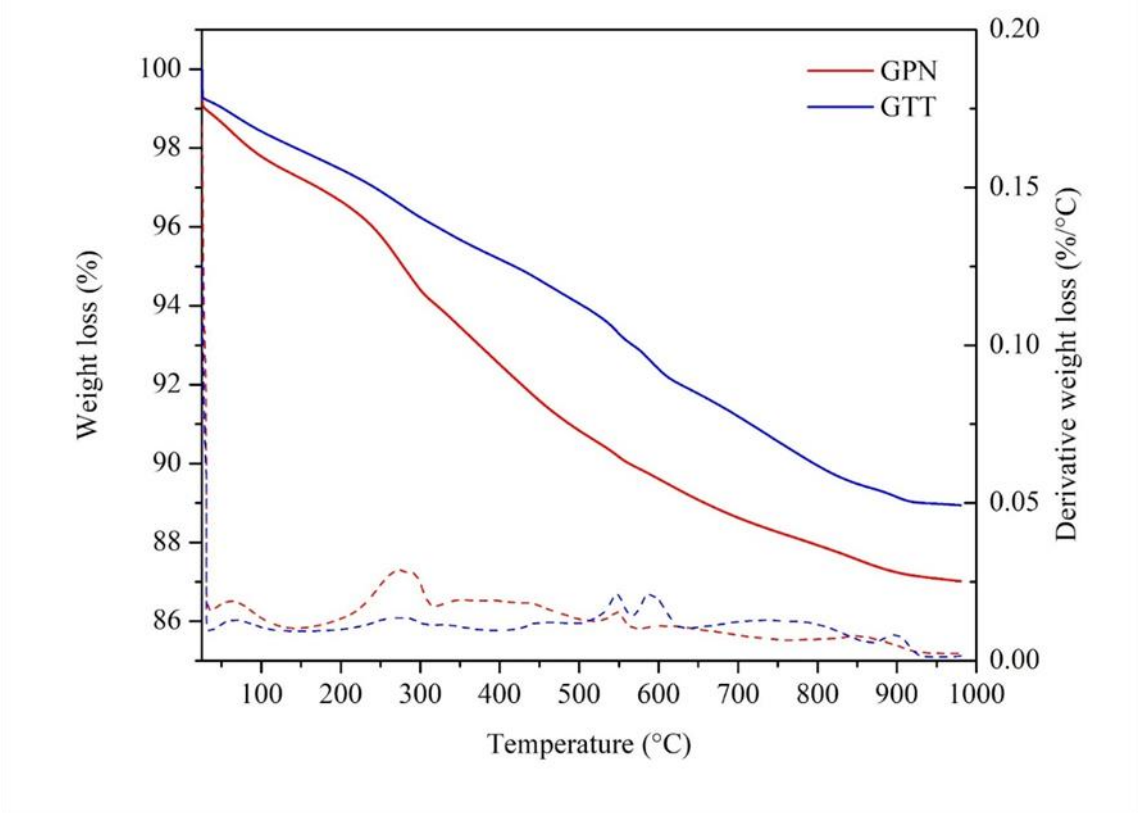

The samples exhibit peaks at similar temperature ranges, with differences only in their weight loss values. Specifically, the weight loss was 12.9% for the GPN sample and 10.9% for the GTT sample. The minor variations could be attributed to the small mineralogical variability between the samples. The weight loss from room temperature to 200 °C was related to moisture loss. In the temperature range of 200–450°C, the weight loss could be attributed to the elimination of structural water from the todorokite, goethite, and epidote hydrated phases. Between 450 and 600°C, the decomposition of todorokite into mineral type α-Mn_3O_4 (possibly hausmannite) occurs, along with the beginning of the decomposition of pyrolusite and cryptomelane into minerals of type α-Mn_2O_3. From 600 to 850°C, the decomposition of pyrolusite and cryptomelane into minerals of type α-Mn_2O_3 (possibly braunite and/or bixbyite) takes place, along with the decomposition of dolomite through the loss of CO_2 in a gaseous state and the formation of calcite. Finally, from 850 to 1000°C, the decomposition of minerals of type α-Mn_2O_3 into minerals of type α-Mn_3O_4 (possibly hausmannite) occurs.

Drumming

Table 3 provides a comparative analysis of the drumming test results for GTT and GPN samples. Both lump ore samples exhibited progressive increases in the formation of fines across all granulometric ranges as drumming time increased. The highest degradation rates were observed at the 6.3 mm range, likely due to the combined effects of the greater impact forces exerted by larger particles and the inherent fragility of their highly porous surfaces.

Table 3 - Drumming results for GTT and GPN manganese ores samples

Size (mm)	Time (min)	GTT (%)	GPN (%)
	10	4.10	3.90
CGD (-6.300)	20	6.40	5.80
	30	7.90	7.30
	10	1.80	1.50
CGD (-0.500)	20	2.80	2.40
	30	3.30	2.90
	10	1.60	1.20
CGD (-0.150)	20	2.30	1.70
	30	2.70	2.00

Decrepitation

Figure 3 and 4 presents the decrepitation index results for the three main sizes of the samples under the studied conditions. The decrepitation indices were highest in the 6.3 mm range, indicating that the generation of fines primarily originated from the coarse fraction of the lump ore samples. According to Faria et al. (2012), the production of fines due to the fragility of the coarse fraction is likely caused by rapid and catastrophic ruptures in the particles. These ruptures may be related to the elimination of structural water and the presence of induced stresses within the particles.

GPN exhibited lower degradation rates during heating compared to GTT under the conditions of drying and heat treatment. Ores with high porosity and pore volume facilitate the release of water vapor and other gases, meaning that a higher presence of

pores results in greater internal pressure relief within the particles (Faria et al. 2012; Faria et al. 2013). For GTT, the significant increases in vapor pressure, combined with lower porosity and a smaller total pore volume, likely caused more abrupt particle ruptures, and, consequently, a greater generation of fines.

The decrepitation results also revealed that all decrepitation indices were lower for dried or heat-treated samples compared to those in their natural state. The higher decrepitation indices in the natural state are attributed to moisture, as the water vapor generated during heating exerts pressure on the pores and particle walls, leading to increased decrepitation.

A reduction of 31% was observed in GTT when dried at 105°C and 27% when heat treated at 200°C. For GPN, the reductions were 43% and 35%, respectively. In both samples, the greatest reduction was achieved in those that were only dried. The high porosity of the two samples, along with the presence of hydrated minerals such as todorokite and goethite, likely explains the increased production of fines.

Figure 3 - Decrepitation indices for the GTT sample

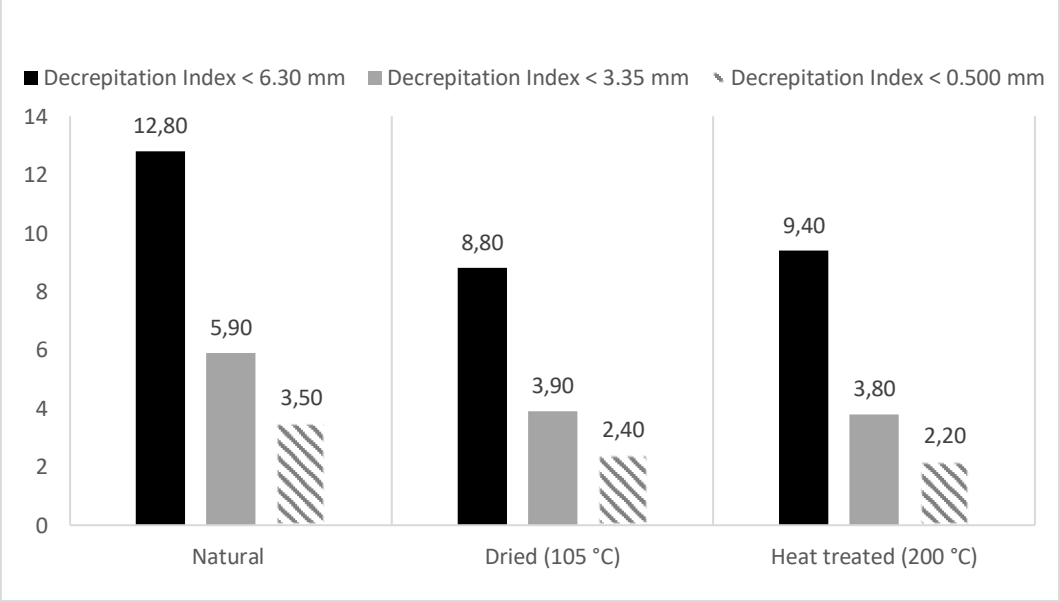

Figure 4 - Decrepitation indices for the GPN sample

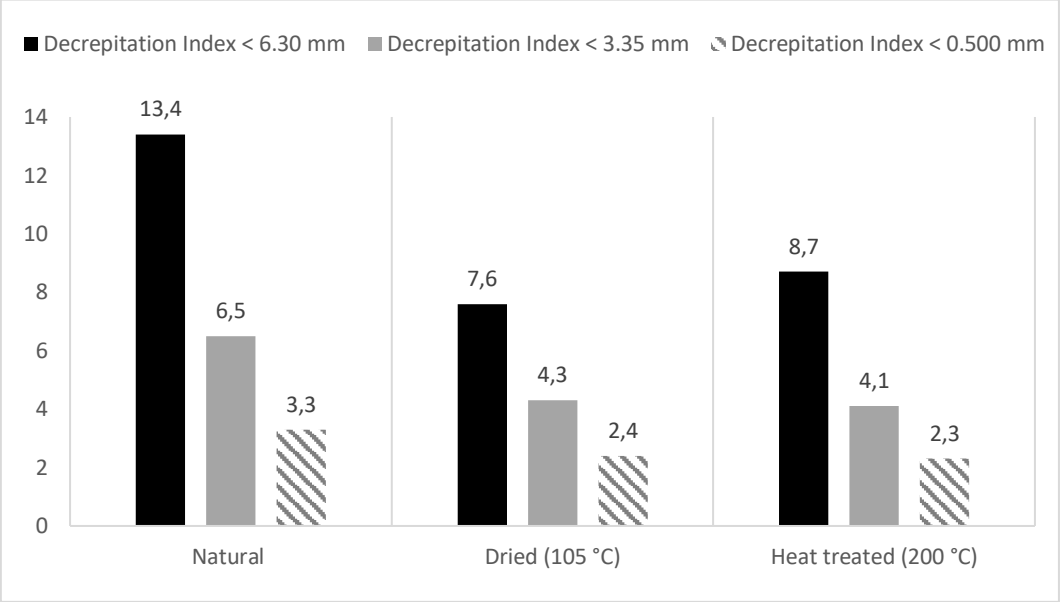

CONCLUSIONS

The analyzed manganese ore samples displayed significant chemical composition variations, with varying levels of manganese, iron, and silica between the GTT and GPN samples. The disparity in the manganese-to-iron ratio (Mn/Fe) indicates the potential for blending ores from diverse sources to achieve the desired ratio and effectively regulate elements such as silica, alumina, and phosphorus. High silica values in the samples suggests their potential suitability for application in SiMn production. The main crystalline phases identified in both samples were spessartite, todorokite, pyrolusite, cryptomelane, quartz, dolomite, and goethite. The GPN sample had a higher specific surface area, porosity, and total pore volume than the GTT sample, indicating possible differences in geological characteristics. Thermogravimetry analysis showed mass losses due to the elimination of structural water from hydrated todorokite and goethite, thermal decomposition of pyrolusite and cryptomelane oxides, and the decomposition of calcium and magnesium carbonate from dolomite. Drumming and decrepitation tests revealed a tendency towards fines generation in both samples, likely due to high porosity and the presence of hydrated minerals. The highest cold granulometric degradation indexes were observed in the 6.3 mm, likely due to the intense impact forces from larger particles and the fragility of their surfaces caused by high porosity. Decrepitation indexes were also higher in the 6.3 mm. The susceptibility to fines production in this size range is likely due to rapid and catastrophic particle ruptures related to the elimination of structural water

and induced stresses. The decrepitation tests indicated that moisture significantly influences fines production. Heat treatment reduced the decrepitation index in the (- 6,3 mm) size range by 27% for GTT and 35% for GPN.

ACKNOWLEDGMENTS

The authors acknowledge the financial support provided by CNPq, FAPEMIG, PROPP/UFOP, and CAPES.

REFERENCES

BERG, K. L.; OLSEN, S. E. Kinetics of manganese ore reduction by carbon monoxide. Metallurgical and Materials Transactions B, v. 31, n. 3, p. 477–490, 2000.

CHEMALE Jr., F.; TAKEHARA, L. Minério de Ferro: Geologia e Geometalurgia. São Paulo: Editora Edgard Blucher Ltda, 2013, p. 178-188.

CHERAGHI, A.; BECKER, H.; EFTEKHARI, H.; YOOZBASHIZADEH. SAFARIAN, J. Characterization and calcination behavior of a low-grade manganese ore. Materials Today Communications, v. 25, p. 101382, 2020.

COETSEE, T.; REINKE, C.; NELL, J.; PISTORIUS, P. Reduction Mechanisms in Manganese Ore Reduction. Metallurgical and Materials Transactions B, v. 46, n. 6, p. 2534–2552, 2015.

COTA, T. G.; CHELONI, L. M. D. M. S.; GUEDES, J. J. M.; REIS, É. L. Silico-manganese slag and its utilization into alkali-activated materials: A critical review. Construction and Building Materials, v. 399, p. 132589, 2023.

DIGERNES, M. N.; RUDI, L.; ANDERSSON, H.; MAGNUS, S.; WASBØ, S. O.; KNUDSEN, B. R. Global optimization of multi-plant manganese alloy production. Computers and Chemical Engineering, n.110, p. 78–92, 2018.

FARIA, G. L.; REIS, E.L.; ARAUJO, F. G. S.; VIEIRA, C. B.; KRUGER, F. L.; JANNOTI Jr., N. Characterization of manganese alloy residues for the recycling of FeSiMn and high-carbon FeMn fines. Materials Research, v.11, p. 405-408, 2008.
FARIA, G. L.; VIANNA, N. C. S.; JANNOTI Jr., N.; VIEIRA, C. B.; ARAUJO, F. G. S. Decrepitation of Brazilian Manganese Lump Ores. In: THE TWELFTH INTERNATIONAL FERROALLOYS CONGRESS, INFACON XII, Helsinki, 2010, p. 449-456.

FARIA, G. L; JANNOTTI Jr., N.; ARAUJO, F. G. Decrepitation behavior of manganese lump ores. International Journal of Mineral Processing, v. 102, 2011.

FARIA, G. L; REIS, E. L.; JANOTTI Jr., N.; ARAÚJO, F. G. S. Caracterização química, física e mineralógica do produto granulado de manganês proveniente da Mina do Azul. Revista Matéria, v.17, n.1, p. 901-908, 2012

FARIA, G. L. et al. Disintegration on heating of a Brazilian manganese lump ore. International Journal of Mineral Processing, v. 124, p. 132–137, 2013.

GRISHCHENKO, S. G.; KRIVENKO, V. V.; OVCHARUK, A. N.; OLSHANSKY, V.I.; FILIPPOV, I. The Comprehensive Analysis of Physical and Chemical Properties and Metallurgical Value of Foreign Manganese Raw Materials Used During Ferroalloy Production. In: THE FOURTEENTH INTERNATIONAL FERROALLOYS CONGRESS, Kiev, Ukraine, 2015, p. 446-453.

INTERNATIONAL MANGANESE INSTITUTE (IMnI), 2008-2016. IMnI annual review. www.manganese.org

LIU, B.; ZHANG, Y.; LU, M.; SU, Z. LI, G.; JIANG, T. Extraction and separation of manganese and iron from ferruginous manganese ores: A review. Minerals Engineering, v. 131, p. 286–303, 2019.

NAVARRO, G. R. B.; ZANARDO, A. Tabelas para determinação de minerais. 1. ed, Rio Claro: Ed. do autor, 2018, v.1, 220p.

OLSEN, S. E.; TANGSTAD, M.; LINDSTAD, T. Production of Manganese Ferroalloys. SINTEF and Tapir Academic Press, Trondheim, 2007, 247 p.

PETERSON, M. J.; MANUEL, J. R.; HAPUGODA, S. Geometallurgical characterisation of Mn ores. Applied Earth Science, v. 130, n. 1, p. 2–22, 2021.

PORPHÍRIO, N. H.; BARBOSA, M. I. M.; BERTOLINO, L. C. Caracterização Mineralógica de Minérios (Parte I). In: LUZ, A.B. Tratamento de Minérios, 5. ed, Rio de Janeiro : CETEM/MCT, p.57-84, 2010.

REIS, E. L.; FARIA, G. L.; ARAUJO, F. G. S.; TENORIO, J. S.; VIEIRA, C. B.; JANNOTI Jr., N. Caracterização de uma Tipologia de Minério de Manganês do Brasil. Revista Escola de Minas, v.63, n.3, p. 517-521, 2010.

RINGDALEN, E.; TANGSTAD, M.; BRYNJULFSEN, T. Melting Behaviour Of Mn Sources-Effect On Furnace Performance. In: THE FOURTEENTH INTERNATIONAL FERROALLOYS CONGRESS, Kiev, Ukraine, 2015, p.436-445.

SINGH, V.; BISWAS, A.; TRIPATHY, S. K.; CHARTTERJEE, S.; HAKERBORTHY, T. K. Smart ore blending methodology for ferromanganese production process. Ironmaking and Steelmaking, v. 43, 2016.

SORENSEN, B; GAAL, S.; RINGDALEN, E.; TANGSTAD, M.; KONONOV, R.; OSTROVSKI, O. Phase compositions of manganese ores and their change in the process of calcination. International Journal of Mineral Processing, v. 94, n. 3, p. 101– 110, 2010.

TANGSTAD, M. Manganese Ferroalloys Technology. In: Handbook of Ferroalloys. [s.l: s.n.]. p. 221–266, 2013.

ULLMANN, F. Manganese and Manganese Alloys. In: Encyclopedia of Industrial Chemistry. 5.ed, Weinhein, Germany: VCH, v.16 A, p. 77-133, 1985.

VIANA, N. C. S. Mineralogia, Calcinação e Nova Classificação Tipológica de Minérios de Manganês Sílico-Carbonatados. 2009. 157p. Dissertação (Mestrado). Programa de Pós - Graduação em Engenharia de Materiais, Rede Temática em Engenharia de Materiais, Universidade Federal de Outo Preto, Ouro Preto.